The Astrophysical Journal Supplement Series, 183:225–243, 2009 August doi:10.1088/0004-637X/183/2/225

A CATALOG OF CORONAL "EIT WAVE" TRANSIENTS

B. J. Thompson[1] and D. C. Myers[2]
[1] NASA Goddard Space Flight Center, Greenbelt, MD 20771, USA
[2] Adnet Systems, Rockville, MD, USA
Received 2004 June 15; accepted 2005 April 6; published 2009 July 23

ABSTRACT

Solar and Heliospheric Observatory (*SOHO*) Extreme ultraviolet Imaging Telescope (EIT) data have been visually searched for coronal "EIT wave" transients over the period beginning from 1997 March 24 and extending through 1998 June 24. The dates covered start at the beginning of regular high-cadence (more than 1 image every 20 minutes) observations, ending at the four-month interruption of *SOHO* observations in mid-1998. One hundred and seventy six events are included in this catalog. The observations range from "candidate" events, which were either weak or had insufficient data coverage, to events which were well defined and were clearly distinguishable in the data. Included in the catalog are times of the EIT images in which the events are observed, diagrams indicating the observed locations of the wave fronts and associated active regions, and the speeds of the wave fronts. The measured speeds of the wave fronts varied from less than 50 to over 700 km s^{-1} with "typical" speeds of 200–400 km s^{-1}.

Key words: Sun: corona – Sun: UV radiation – waves

1. INTRODUCTION

Coronal "Extreme ultraviolet Imaging Telescope (EIT) wave" transients are typically observed as moving fronts of increased coronal EUV emission, traveling at the speeds of a few hundred km s^{-1} (Dere et al. 1997; Thompson et al. 1998, 1999). They are usually faint (<20% increase in emission), are fairly large in scale (a few arcminutes in thickness, with angular spans ranging from a few arcminutes to over a solar radius), and can propagate across the entire observable disk of the Sun. These disturbances can be weak, down to the limit of observability (<10% of pre-event emission), or they can be extremely bright, reaching a threefold increase in emission (e.g., Thompson et al. 2000).

EIT waves have been observed to have a wide range of speeds, from less than 200 km s^{-1} to inferred speeds near 1000 km s^{-1}. Because the typical EIT image cadence is 9 to 17 minutes, extremely fast or short-lived waves are difficult to detect with the EIT alone. Higher-cadence imagers such as *Transition Region and Coronal Explorer* (*TRACE*; Handy et al. 1999) are able to view the evolution much more clearly. Wills-Davey & Thompson (1999) describe an EIT wave with 1 minute *TRACE* observations revealing the EIT wave's magnetohydrodynamics (MHD)-wave-like propagation and refraction in relation to the magnetic structures (see also Wang 2000). Multiple views from STEREO SECCHI (Howard et al. 2008) have dramatically improved our ability to observe the phenomenon in a three-dimensional context (Long et al. 2008; Ma et al. 2009). Wu et al. (2001) and Ofman & Thompson (2002), following the seminal work of Uchida (1968, 1970, 1974), have demonstrated that computational MHD simulations are capable of reproducing many of the physical properties of these phenomena.

It has been demonstrated (Thompson et al. 2000; Warmuth et al. 2001; Pohjolainen et al. 2001; Eto et al. 2002) that some (a small fraction) of the EIT waves can display accompanying Hα transients, known as Moreton waves (Moreton 1960; Moreton & Ramsey 1960) or flare-associated waves (Smith & Harvey 1971). Hα Moreton wave comparisons with EIT wave observations (Thompson et al. 2000; Warmuth et al. 2001, 2004a, 2004b; Pohjolainen et al. 2001; Vršnak et al. 2002) have led to a greater understanding of the development of large-scale waves on the Sun. However, there is continued debate regarding the relationship between EIT waves and Hα waves (Eto et al. 2002; Chen et al. 2002; Warmuth et al. 2004a, 2004b). Zhukov & Auchere (2004) investigated the relationship between EIT waves, EUV dimmings and coronal mass ejections (CMEs) using EIT data from multiple wavebands, in particular the 284 Å bandpass. Their close examination of two EIT wave events reveals that the waves may exhibit separate "eruptive" and "wave" modes, corresponding to different origins of the EUV brightening. The events listed in this catalog were all derived from the EIT 195 Å observations, and we only demarcate moving bright fronts and do not distinguish between the different proposed sources of increased emission.

This catalog consists of events determined by visual inspection of data, and not by an automated technique. Recent efforts at developing automated computational algorithms to detect EIT waves show promise. In particular, the Novel EIT Wave Machine Observing algorithm (Podladchikova & Berghmans 2005) is providing automated updates for the STEREO mission, and Wills-Davey (2006) has implemented a tracking technique that provides more comprehensive statistics for wave propagation studies. These algorithms offer three advantages: the results are consistent and reproducible, the search algorithm requires less labor than a manual search, and an automated search can produce results in near-real time. A direct comparison between this catalog and the results of automated search algorithms is not within the scope of this paper. However, this comparison would be necessary to truly determine the relative strengths and limitations of the different approaches. A recent review by Banerjee et al. (2007) discusses a number of detection approaches used in the study of "Atmospheric Magnetoseismology."

The EIT (Delaboudinière et al. 1995) is a normal-incidence, multilayer EUV telescope aboard the *SOHO* spacecraft. In its nominal observing mode, EIT obtains a series of full-frame (44.2 by 44.2 arcmin) images in a bandpass dominated by the emission lines of Fe XII at 192.3, 193.5, and 195.1 Å. The Fe XII emission lines exhibit a peak emission near 1.5 MK at coronal densities. (Note: other emission lines are capable of contributing to this bandpass. We are unable to separate these lines using the EIT data alone, but the majority of the typical coronal emission comes from the Fe XII lines. However, the

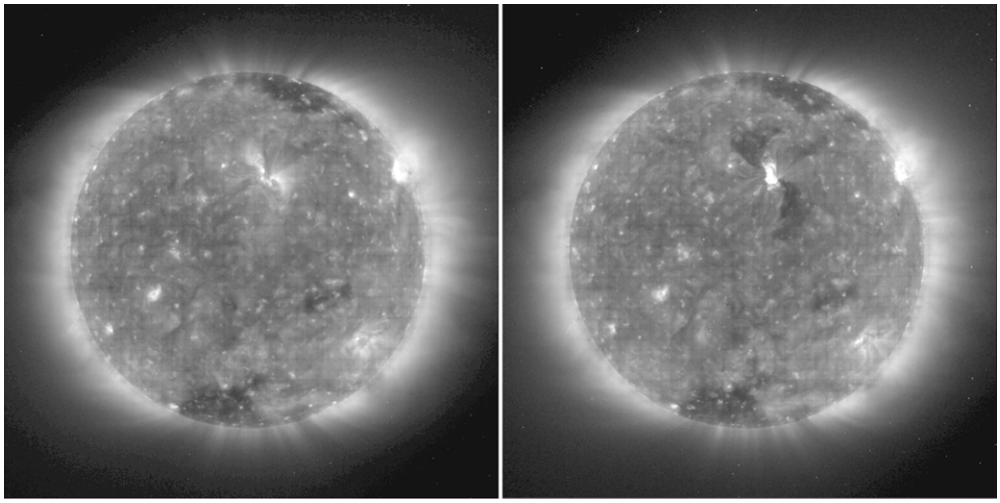

Figure 1. Two EIT 195 Å images taken on 1997 May 12 at 01:12 (left image) and 06:49 UT (right), before and after the EIT wave event.

wave fronts described in this catalog may not necessarily consist exclusively of changes in Fe XII emission; this may influence the interpretation of the wave properties but not the measurements in this catalog.) In this paper, we refer to the logarithmically scaled data from this bandpass as "195 Å images," and for most of 1997 and 1998 EIT was obtaining 195 Å half- or full-resolution images at cadences of 9–17 minutes. The pixel scale of full-resolution images is 2.59 arcsec, while half-resolution "2 × 2" binned images have a pixel scale of 5.18 arcsec. Both the full- and half-resolution images were examined in compiling this catalog.

The waves are most easily observed when the images have been enhanced digitally, or processed in a way that highlights the changing aspects of the corona. The three ways we viewed the wave events are: (1) logarithmically scaled images, (2) images with a pre-event "base" image subtracted from them, and (3) "running-difference" images. In general, it is difficult to distinguish EIT waves in movies of logarithmically scaled, raw (unsubtracted) images; the changes in the corona are generally too faint to detect without an enhancement technique. Base differencing, where the same pre-event image is subtracted from a series of images, is generally sufficient to detect well-defined events. However, the base-differencing technique has less utility when the time between the two images is greater than half an hour; other emission and structural changes in the corona can dominate. The faintest waves can only be detected via running-difference images, where a movie is made of images from which the immediately preceding "raw" image has been subtracted. This technique emphasizes frame-to-frame images, making it easier to detect weak events.

A running-difference image can be viewed, in essence, as an approximation of the "time derivative" of the changing emission in the corona. An image pixel that has no or little change in emission between the two images will appear as a gray pixel after the difference has been scaled and represented in a black–gray–white color table, where the white end of the spectrum represents an increase in emission since the previous image, and the black end of the spectrum denotes a decrease. It is important to note the following caveat: running-difference images only represent the net change in emission. For example, if Region "A" is 10 times brighter than region "B", then region "A" only needs to show a 10% change in emission to register the same change as a doubling of the emission in region "B." Additionally, if region "C" shows an increase in emission, which later returns to its original value, the difference images will show a brightened area, followed by a darkened area in the next difference. Running-difference images can be deceptive, in that a darkened area merely indicate an area that has decreased in emission *since the previous image.* Therefore, darkened areas in running-difference images can be due to regions, which are "newly darkened" or which were "previously brightened."

Thompson et al. (1998) describe a propagating increase in EUV emission on 1997 May 12 that encircles a flaring active region. The speed of the transient was in excess of 200 km s^{-1}, and in less than an hour the wave was no longer visible, and had either faded or propagated beyond observability. Figure 1 compares EIT 195 Å images from 01:12 to 06:49 UT, before and after the observation of the 1997 May 12 wave transient. The active region, in the northern hemisphere, shows bright flare loops and the development of "dimming" areas (regions of coronal depletion associated with a coronal mass ejection) to the north and south of the region. The primary contribution of flux near 195 Å is from Fe XII, which represents a temperature near 1.5 MK at coronal densities. While the flare and the dimming regions are visible in these images, the wave's transit leaves no clear aftereffects in the surrounding corona.

Figure 2 shows a series of images from the 1997 May 12 event, as a series of running differences, where each image has the previous image digitally subtracted from it. The first (second) panel shows the difference between the first (second) two images in Figure 2, with white (black) areas representing an increase (decrease) in emission relative to the previous image. In this case, the wave front is easily observable as a disturbance propagating over nearly the whole solar disk. However, other forms of dynamic activity are visible in the same data. Based solely on the running-difference images, it is difficult to distinguish a propagating transient impulse from other evolving features, such as flares, dimming regions, and CMEs.

Because the EIT wave transients are frequently accompanied by other phenomena, it is important to examine both the unsubtracted 195 Å data and the running-difference images to determine the true locations of wave transients. In particular, the second panel in Figure 2 (05:05 UT) shows a bright circular front encircling a dark area. Examining the third panel (05:22 UT), it is clear that the location of the bright front at 05:05 UT appears

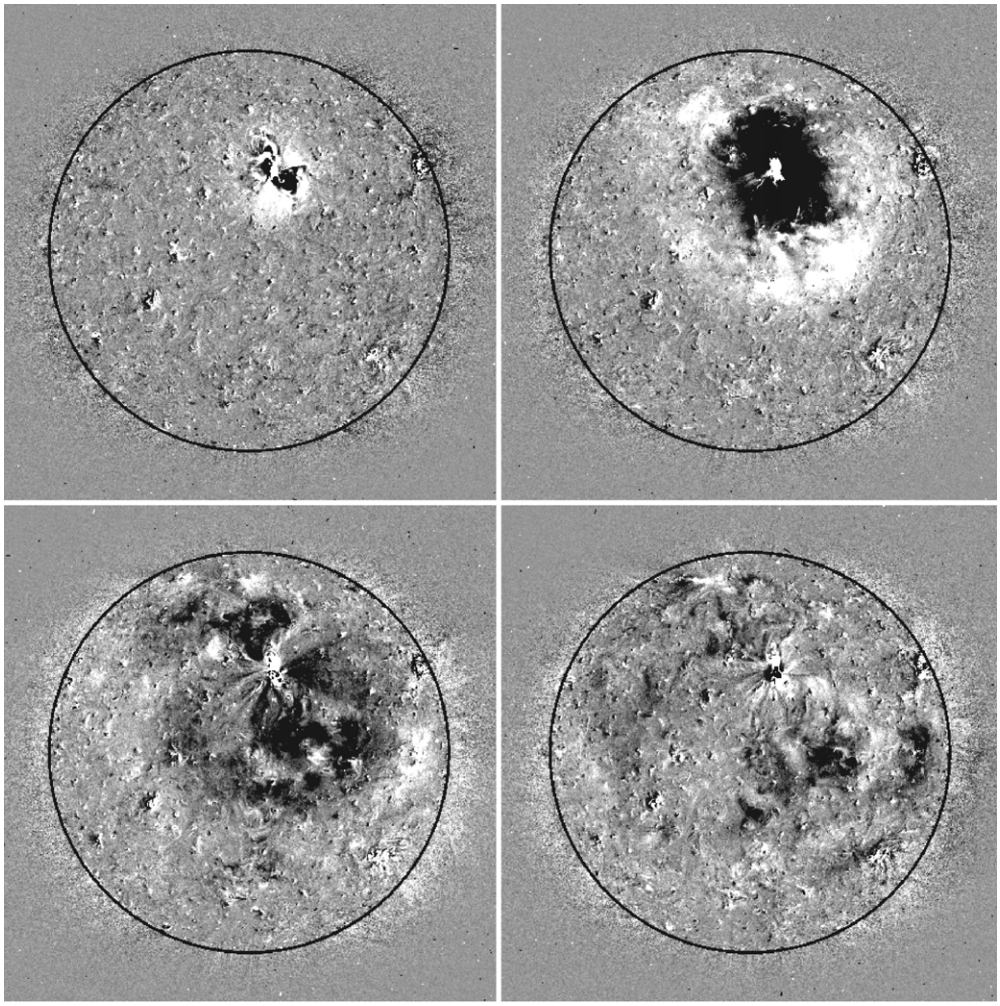

Figure 2. Series of running-difference images for an EIT wave on 1997 May 12. The first frame shows an image at 04:33 UT subtracted from an image at 04:48 UT. The other three image times are 05:05, 05:22 and 05:39 UT. Reprinted from Thompson et al. (1998) with permission from Geophysical Research Letters.

dark at 05:22 UT. However, this does not indicate that the region was bright at 05:05 and then was dark at 05:22; the region has simply returned to a value closer to its initial brightness. We use the running differences to make the location of the wave fronts more visible, but simultaneous examination of the undifferenced 195 Å images is required to determine whether we are tracking a transient bright front.

After viewing a series of undifferenced 195 Å images side-by-side with the running-difference images, the authors derived the location of the wave front by visually identifying the leading edges of the transients. For example, in the second frame of Figure 2, the leading edge of the brightened disturbance is fairly easy to distinguish. However, by the third frame, the leading edge is less clear, and there is great ambiguity in the final frame. Because the wave fronts were determined in such an "organic" matter, we developed a catalog that reflects our certainty that the emission disturbances we describe are truly propagating wave transients.

2. CATALOG CONTENTS

The catalog consists of all of the observations in the EIT 195 Å images, from January 1996 through June 1998, in which we were able to find evidence of EIT wave-like phenomena. Because the observations are not sufficient to determine whether a transient meets certain physical criteria (such as clear evidence of MHD wave propagation), we include all events that show some evidence, however small, of a propagating transient bright front.

Because EIT waves typically have low amplitudes (less than 20% increase in brightness), and because the background coronal emission can vary greatly in 20 minutes, it is difficult to detect EIT waves in images whose observation times are separated by more than 20 minutes. Therefore, EIT wave events in this catalog were observed in EIT 195 Å images with cadences typically between 9 and 17 minutes.

It is important to note that for every well-observed, high-amplitude wave front generated in the corona, it is very likely that there were many more wave fronts with much smaller amplitudes. Taking this into consideration, it is unreasonable to assume that the EIT waves listed in this catalog, i.e., those that have sufficient amplitude to be observed in the EIT images, represent the entire population of these phenomena. It is more likely that the event amplitudes, if it were possible to perform accurate measurements, would obey a power law, and that for every clearly resolved observation there are an order of magnitude more observations that are much weaker.

Therefore, a lack of an entry in this catalog should not be construed as an absence of wave activity. In many cases, there was not a sufficient number EIT images to identify the presence of a wave. Additionally, there are undoubtedly many cases of

Table 1
Table Entries for the First Two Entries in the Wave Catalog, Corresponding to the Figures Shown in Figure 3

	Date	Quality Rating	Source Location N/S	Source Location E/W	Previous Image Time	Image Time	Speed Plane of Sky	Speed Projected	Direction of Meas.
1	1997 Mar 25	Q0	2	−58	1:42:33	**1:59:35**			NW
						2:17:28	63	88	
2	1997 Apr 1	Q1	−25	−16	5:02:43	**5:21:13**			NW
						5:33:56	280	291	
						5:43:08	290	301	

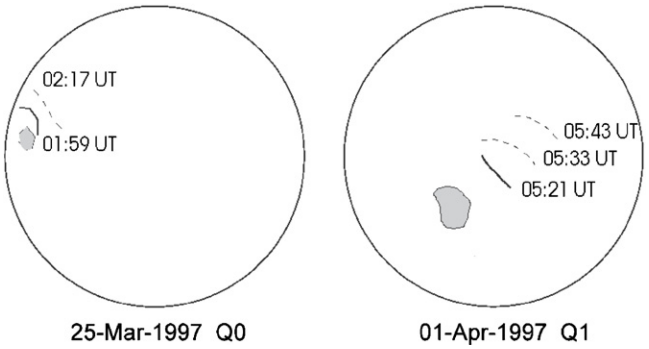

Figure 3. First two entries in the wave catalog, corresponding to the entries shown in Table 1.

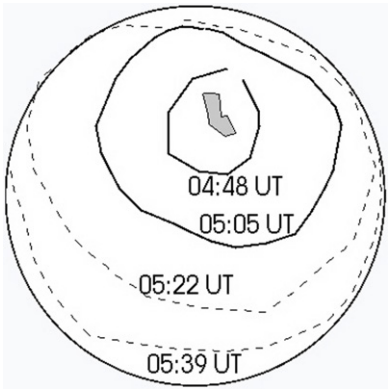

Figure 4. Wave diagram for 1997 May 12 EIT wave catalog entry.

waves that are either too faint or too short-lived to have been identified in the data by the authors. As mentioned previously, EIT waves are most easily viewed in images obtained at a relatively fast cadence (around 10 minutes) against the "quiet Sun" (devoid of active regions, coronal holes, filament channels and other magnetic features).

During periods with high-cadence EIT images, and a background corona that is relatively quiet, it is highly unlikely that a clear "Q4- or Q5-quality" event would be missing from the catalog. However, there were many times when the observations were less than optimal, particularly when the image cadence was insufficient. There is only one entry in the catalog (1998 April 21) that spans more than an hour. Therefore, the detection of an EIT wave depends on the availability of multiple images over timescales of less than one hour.

Again, we stress that this catalog is not meant to be viewed as a complete listing on wave disturbances, but we aimed to make the listing as comprehensive as possible. Depending on the research performed with this catalog, a wave transient that is missing from the catalog may have no significance, or it may skew the conclusions of a study. We encourage the reader to take into consideration the wave observability factors when using the catalog for their own scientific studies.

The first two catalog entries are shown in Figure 3 and Table 1. A detailed description of each of the sections of the catalog follows.

2.1. Wave Diagrams

A summary image, or diagram, is included for each entry in the catalog. The summary images consist of a gray region identifying the source or associated active region (if any), and lines indicating the locations of the leading edge of the wave front at each of the image times. When the location of the leading edge of the wave front is relatively clear, we use a solid black line. When the location is difficult to resolve, or when it is not clear whether the change in emission is a continuation of a previous wave location, we indicate the uncertainty with a dashed line. Frequently, the wave diagrams will consist of solid lines early in the event, fading to a dashed line at later times. This distinction has been drawn to provide greater information about the events, and users of the catalog are encouraged to make note of the difference between the solid-lined "good" wave fronts, and the dashed-lined "sketchy" locations.

Figure 4 shows the catalog wave diagram for the 1997 May 12 EIT wave. The limb of the Sun is outlined in the figure, and the associated active region is shown by the outlined gray area in the center. The wave fronts that were visible in Figure 2 are drawn on the diagram, along with the image times at which each of the fronts were observed. A solid line indicates that the wave front had a clear boundary in brightness in the 4:48 and 5:05 UT images (panels 1 and 2 in Figure 2), while the dashed lines show the wave fronts which are not as clear (panels 3 and 4 in Figure 2).

2.2. Date

The "Date" column in the catalog gives the date of the first image showing the wave front. Please note that in cases where the pre-event image listed in the catalog occurs prior to 00:00 UT and the first image occurs after 00:00 UT, the date of the pre-event image is 1 day before the listed date.

2.3. Quality Rating

For the purpose of research that aims to study the association of other phenomena with EIT waves, the catalog must include all of the observed EIT wave events that are detectable in the available EIT data using our identification technique, even those which are so weak or so poorly observed that there is a low probability that the event is an actual wave. Still, many studies looking for direct links between EIT waves and associated phenomena would benefit from relying only on those events which are almost "definitely" waves. To resolve this issue, we have introduced a "Quality Rating," which we assign to each

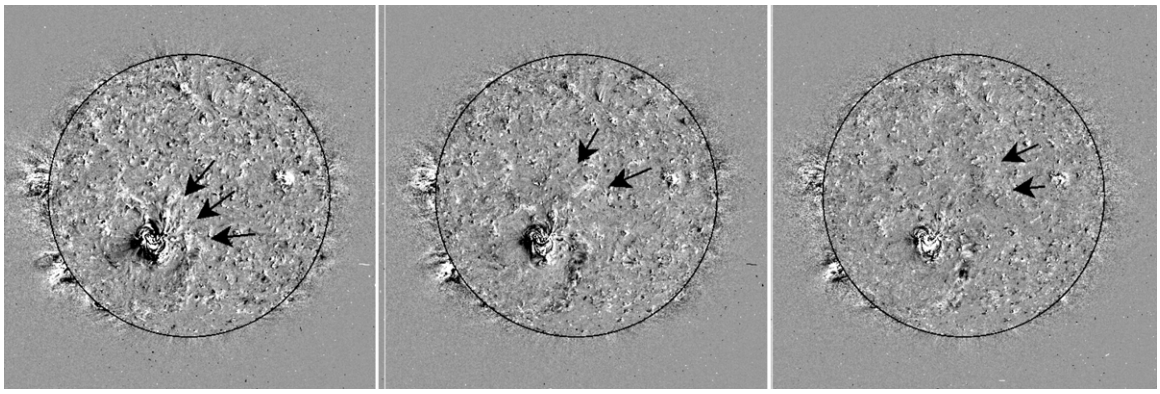

Figure 5. Running-difference images of 1997 April 1 event. The first image is the difference between the images at 05:21 and 05:03 UT, while the second and third images were taken at 05:33 and 05:43 UT. Arrows indicate the locations of the brightenings. This is an example of a catalog entry with a quality rating of "Q1."

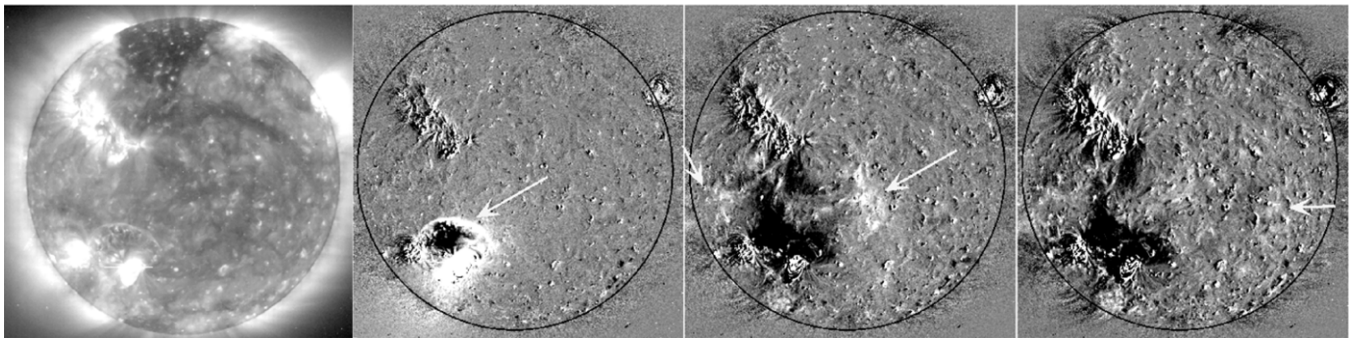

Figure 6. First panel shows an EIT image with a sharp bright front on 1997 September 24 at 02:49 UT. The three following panels show EIT images taken at 02:49, 03:03 and 03:23 UT with a pre-event image at 02:32 UT digitally subtracted from them. White arrows indicate the progression of the EIT wavefronts. Adapted from Thompson et al. (2000) with permission from Solar Physics.

event. The Quality Rating is an indicator of the observability of the wave in the data.

The Quality Rating is a subjective parameter, and it does not depend solely on wave amplitude or brightness. A wave may be difficult to distinguish for several reasons: (1) the wave is extremely faint (less than the typical 5%–10% change in emission), (2) the time between the images is larger than average, and the change in emission in the background corona has begun to "wash out" the change in emission due to the wave, (3) there are few (one or two) images showing the wave, and/or (4) the wave is propagating through a region of highly structured corona, where a faint change in emission is difficult to observe against the background features. Although high-amplitude, long-range waves propagating against a "quiet" background tend to be assigned a higher Quality Rating, the authors ultimately based the Quality Rating on the ease with which they were able to identify and outline a propagating wave front.

The Quality Rating Scale, described in Table 2, ranges from "Q0" to "Q5". These ratings can be used an indicator of our confidence that the transient event observed is "really" an EIT wave. As a rough guide, we have assigned a value to our degree of confidence for each Quality Rating, shown in the column labeled "Confidence Level." This value is *highly subjective*, indicating to the reader that we suspect, based on our experience in viewing EIT waves, that many of the "Q0" and "Q1" catalog entries are "false positives."

For example, cases with a rating of "Q0" typically were events that were extremely weak or had poor data coverage. It may be possible that a large number of the events that received low-quality ratings do not have the physical properties of an EIT wave at all and are transient brightenings due to an entirely different process. A "Q5" rating refers to those transients that

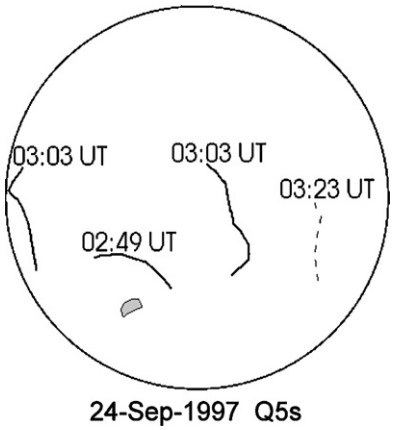

Figure 7. Wave diagram for the catalog entry for the 1997 September 24 event shown in Figure 6.

were well defined and clearly visible in the data. Again, it is important to note that this classification scheme is not a unique indicator of the intensity or speed of a wave. However, the visibility of a wave, and thus its quality rating, is likely to depend on these to at least some extent.

The 1997 May 12 wave event shown in Figures 1, 2, and 4 is an example of a catalog entry receiving a "Q5" rating. However, the majority of the entries receive a rating of Q3 or lower. Figure 5 shows the running-difference images corresponding to the wave diagram of the 1997 April 1 event shown in Figure 4. Arrows show the location of the alleged wave fronts, which are not nearly as clear as the wave fronts in Figure 2. This is an example of a "Q1" event. This event has been included in the catalog only because some studies may derive value from

Table 2
Wave Quality Ratings, Defined With Respect to The Wave's Observability in The EIT Data

Quality Rating	Description/Criteria	Confidence Level (%)	No. of Events
Q0	Very low reliability; either a bright front with no clear evidence of propagation, an extremely faint disturbance, or unusual structure. We suspect that this category includes a number of weak waves as well as non-related phenomena	<10%	37
Q1	Low reliability; either a faint bright front with structure which may resemble those in the class 5 events, or some evidence of a propagating brightening	10%–25%	54
Q2	Low reliability; faint to strong bright front or a brightening which is moving	25%–50%	39
Q3	Intermediate reliability; Either multiple images of a propagating brightening, or a clear observation of a bright front which is very similar in structure to the class 5 waves	50%–75%	25
Q4	High reliability; Multiple images of a propagating brightening, spatial correspondence from one image to the next, fairly high reliability	>75%	16
Q5	Nearly definite reliability; Clear evidence of a propagating bright front in multiple images, extent of the wave is far from other activity such that the transient increase in emission is able to be distinguished from other evolving features	100%	5

Notes. The confidence level should be treated as a *rough* probability that the observation is a propagating MHD wave. The number of events listed in the last column indicate how many of the entries in the catalog (out of 176) are in each category.

knowing all possible events. However, it is clear that the events with higher Quality Ratings are much more suitable for detailed studies of wave propagation.

Most of the events in the catalog consist of diffuse brightenings of relatively low amplitude. However, a small fraction of the EIT waves (7%) had sharp, bright components associated with them. The majority of the observations of sharp waves, which are designated with an "S" in their rating (e.g., Q4 S), also exhibit the more typical diffuse brightenings in later images. An example of an EIT wave from 1997 September 24 that exhibits both diffuse and sharp features is shown in Figure 6 and diagrammed in Figure 7, which are adapted from Thompson et al. (2000). The first panel shows an undifferenced image taken at 02:49 UT, showing a bright front or arch forming to the north of a flaring active region. The next three panels show EIT images from 02:49, 03:03, and 03:23 UT with a pre-event image from 02:32 UT digitally differenced from them. Arrows indicate the progress of the EIT wave front(s), though the wave front is faint by the third image and only an approximate location is indicated. There is no evidence of a sharp brightening in the 03:03 and 03:23 UT images, though the diffuse wave fronts continue to be visible.

We stress that these ratings are qualitative; although both authors independently reviewed the rating for each event, the quality number assigned to many events could vary by 1 or 2 between the authors. Researchers looking to perform correlative studies which rely on highly reliable or nearly unambiguous evidence of an EIT wave should restrict their studies to events in the catalog with a high-quality rating. We also encourage researchers who include all waves in the catalog in a study to examine their results relative to the quality rating. For example, Biesecker et al. (2002) compared the occurrence of flares and CMEs with many of the events in this catalog, and found that the correlation with both flares and CMEs increased when the sample was restricted only to the waves with a quality rating of 3 and above.

The authors did attempt to derive a less subjective means of classifying the wave observations. Clearly, the wave amplitude would be an optimal measure, but the increase in emission throughout the wave fronts is not at all homogeneous, and the amplitude decreases drastically with time. The attempts to evaluate a wave amplitude were strongly influenced by the timing of the EIT image and by the size of the area used to assess the wave amplitude. Additionally, this means of classifying the waves did not take into account the events of low-quality rating which we suspect may not be EIT waves, but merely show evidence of a transient brightening of some sort. Some brightenings at coronal hole boundaries or during filament eruptions can resemble a bright arc, and these events frequently display a significant increase in emission. Meanwhile, some of the "good" events have a low amplitude but are easily observable because the transient brightening occurs over a broad coherent scale. Therefore, we arrived at the qualitative means of rating the waves, which is influenced by any bias of the authors but also their experience, to allow the user of the catalog to have an assessment of the certainty that the event is truly a propagating wave. An example of a catalog entry with quality rating is given in Table 1, and the distribution of the ratings for the catalog is given in Table 2.

2.4. Source Location

The next column in the catalog gives the apparent source location of the EIT wave. Typically, the location listed is the heliographic latitude and longitude of an associated flaring/erupting active region, as most of the wave events are observed propagating away from an active region. In the cases where the active region was part of an extended complex, the source location was identified as the location within the complex, which appeared to be exhibiting evolution associated with the flare. For the cases when the wave did not appear to originate at an active region, the source location listed is either an evolving solar feature or an apparently central origination point. A source longitude of 90 or −90 indicates that the apparent source of the wave was either at, above, or possibly behind the solar limb.

Note: the Source Location is only meant to be a rough indicator of the centroid of the wave disturbance, so that users of this catalog are able to determine which active region (if any) is associated with the EIT wave. None of the measurements listed in the catalog are based on the given Source Location field; the speed measurements lists in the catalog are based on locations of the wave fronts, and are not at all influenced by the Source Location.

2.5. Previous Image Time

Of course, a 10 minute average image cadence is not sufficient to determine the time at which the wave was first produced. We are only capable of determining the times during which the wave

Table 3
Full EIT Wave Catalog. The Wave Diagrams Corresponding to these Entries are Shown in Figures 8(a)–(o)

	Date	Quality Rating	Source Location		Previous Image Time	Image Time	Speed		Direction of Measurement
			N/S	E/W			Plane-of-Sky	Projected	
1	1997 Mar 25	Q0	2	−58	1:42:33	**1:59:35**			NW
						2:17:28	63	88	
2	1997 Apr 1	Q1	−25	−16	5:02:43	**5:21:13**			NW
						5:33:56	280	291	
						5:43:08	290	301	
3	1997 Apr 1	Q1	−25	−16	8:01:51	8:14:29			NW
						8:23:40	271	272	
						8:36:51	231	241	
						8:55:21	128	154	
4	1997 Apr 1	Q0	−25	−15	10:23:51	10:42:24			NW
5	1997 Apr 1	Q4	−25	−11	13:45:17	**13:58:25**			NW
						14:16:51	231	236	
						14:29:30	138	157	
						14:38:44	262	359	
6	1997 Apr 2	Q0	−24	−6	0:44:13	**0:53:31**			NW
						1:06:45	209	216	
7	1997 Apr 2	Q0	−21	6	5:22:09	5:35:21			SW
8	1997 Apr 2	Q0	−21	6	8:56:25	9:09:37			SW
	Note. Wavefront is very weak and uneven at 09:09; possible start time is after 09:09 UT					9:28:08	See note		
9	1997 Apr 6	Q3	−29	−21	23:36:06	**23:48:37**			NW
						23:57:47	184	188	
						0:10:55	122	123	
10	1997 Apr 7	Q5	−29	−20	13:52:49	**14:05:23**			NW
						14:14:34	339	344	
						14:27:45	203	223	
						14:46:12	152	203	
11	1997 Apr 9	Q2	−24	90	11:34:45	11:53:18			N
						12:05:48	295	396	
12	1997 Apr 13	Q1	−30	53	23:05:52	23:14:58			N
						23:28:00	237	238	
						23:46:26	145	off limb	
13	1997 Apr 15	Q2	−23	−15	6:33:06	**6:47:25**			NW
						7:11:00	134	136	
14	1997 Apr 15	Q3	−23	−13	10:11:28	**10:34:21**			N
						10:48:28	256	268	
15	1997 Apr 15	Q4	−23	−9	13:58:28	**14:16:21**			N
						14:34:45	261	264	
						14:49:28	289	334	
						15:16:06	76	127	
16	1997 Apr 16	Q1	−19	−3	14:16:20	**14:34:42**			NE
17	1997 May 9	Q1	20	−29	6:33:25	**6:47:41**			S
						7:11:16	59	61	
						7:32:45	110	110	
18	1997 May 10	Q1	20	−13	13:42:22	**13:59:01**			SW
						14:17:57	183	184	
19	1997 May 12	Q5	22	8	4:33:30	**4:48:49**			S
						5:05:49	244	247	
						5:22:49	235	262	
						5:39:47	157	225	
20	1997 May 15	Q1	22	55	18:26:49	**18:43:39**			S
						19:11:14	56	56	
21	1997 May 25	Q4	−26	−57	14:16:24	**14:33:25**			NW
	Note. Some initial activity in 14:16 image					**14:51:05**	176	194	
						15:07:26	250	253	
22	1997 May 26	Q2	−27	−35	18:40:35	**19:11:14**			NW
						19:24:41	185	190	
23	1997 May 28	Q0	−28	−11	12:18:50	12:39:49			S
	Note. Some initial activity in 12:18 image					13:11:27	141	207	
24	1997 Jun 9	Q1	−32	90	22:28:44	**22:44:00**			N
						23:05:59	205	off limb	
25	1997 Jun 14	Q0	19	−14	23:41:11	23:57:27			N
						0:14:25	48	52	
						0:34:04	29	32	

Table 3
(Continued)

	Date	Quality Rating	Source Location		Previous Image Time	Image Time	Speed		Direction of Measurement
			N/S	E/W			Plane-of-Sky	Projected	
26	1997 Jun 15	Q0	19	−14	3:59:27	4:15:29			NW
27	1997 Jun 18	Q1	29	−90	1:59:25	2:16:25			SW
						2:33:58	116	183	
28	1997 Jun 23	Q0	−29	−90	6:30:24	6:46:50			N
						7:10:11	55	off limb	
						7:23:54	19	off limb	
29	1997 Jun 25	Q2	18	6	23:47:41	**0:07:55**			SE
						0:32:42	129	131	
30	1997 Jun 25	Q0	18	14	14:02:41	14:22:42			SE
						14:48:04	61	62	
31	1997 Jun 29	Q2	18	85	23:38:13	**23:55:13**			S
						0:12:14	229	off limb	
						0:31:46	214	off limb	
32	1997 Jul 4	Q1	−30	−13	2:51:20	3:08:55			SE
						3:24:18	100	209	
33	1997 Jul 8	Q0	−31	90	11:54:39	12:11:40			NW
						12:31:13	101	193	
34	1997 Jul 30	Q1	−34	−36	17:03:38	**17:45:06**			SE
35	1997 Aug 1	Q1	26	20	23:40:39	**23:57:39**			N
36	1997 Aug 3	Q2	7	−62	15:57:29	**16:16:33**			SW
						16:36:15	76	76	
						16:49:28	74	81	
37	1997 Aug 5	Q1	−19	−59	20:50:55	21:08:16			N
						21:29:11	86	off limb	
						21:50:12	67	off limb	
38	1997 Aug 9	Q2	−34	−21	15:55:59	**16:10:03**			S
						16:27:00	53	193	
						16:45:00	72	off limb	
39	1997 Aug 16	Q0	30	−45	18:25:22	**18:38:51**			W
						18:53:52	276	386	
						19:11:22	22	26	
40	1997 Aug 21	Q0	−38	90	0:46:18	1:09:13			N
						1:22:57	321	off limb	
41	1997 Aug 25	Q1	20	−37	0:46:01	**1:09:24**			N
						1:23:06	33	35	
42	1997 Aug 25	Q1	20	30	11:55:23	**12:11:53**			SE
						12:28:54	71	74	
43	1997 Aug 26	Q0	17	−17	9:56:11	10:13:10			S
						10:30:10	46	46	
44	1997 Aug 29	Q2	20	6	4:33:03	**4:57:57**			NW
						5:19:51	82	104	
45	1997 Aug 29	Q0	−23	−16	5:58:03	6:16:08			W
						6:34:14	264	308	
46	1997 Aug 29	Q1	31	−17	23:24:10	**23:40:45**			NE
						23:57:56	61	111	
						0:15:10	58	37	
47	1997 Sep 8	Q0	−28	6	19:39:11	**19:51:04**			NW
						20:05:59	69	78	
						20:27:45	132	160	
48	1997 Sep 9	Q2	40	90	19:13:21	**19:26:22**			S
						19:44:34	151	off limb	
						20:00:04	152	off limb	
						20:18:16	153	off limb	
49	1997 Sep 13	Q3	22	38	19:42:34	**19:59:12**			S
						20:16:29	47	48	
						20:35:58	39	43	
50	1997 Sep 17	Q2	21	85	11:24:10	**11:41:10**			S
						11:58:10	246	off limb	
51	1997 Sep 19	Q1	−21	90	9:24:51	9:41:51			N
						9:58:51	156	off limb	
52	1997 Sep 20	Q4	−16	90	9:41:46	**9:58:47**			N
						10:15:46	144	off limb	
						10:32:47	214	off limb	
53	1997 Sep 22	Q0	−25	−87	0:48:58	1:12:20			N

Table 3
(Continued)

	Date	Quality Rating	Source Location		Previous Image Time	Image Time	Speed		Direction of Measurement
			N/S	E/W			Plane-of-Sky	Projected	
54	1997 Sep 23	Q2	−28	−25	21:23:53	**21:40:46**			N
						21:58:33	193	off limb	
						22:18:09	262	off limb	
55	1997 Sep 24	Q5 S	−28	−22	2:32:41	**2:49:21**			W
						3:03:41	298	410	
						3:23:41	239	264	
56	1997 Sep 24	Q4 S	−29	−19	10:46:03	**11:06:40**			W
						11:29:45	315	325	
						11:39:29	211	251	
57	1997 Sep 24	Q4 S	−28	−13	18:30:31	**18:47:33**			NW
						19:11:05	192	216	
58	1997 Sep 25	Q1	−28	−3	11:39:54	**11:56:54**			N
						12:13:56	184	187	
59	1997 Sep 28	Q4	−26	−90	14:00:33	**14:10:45**			N
						14:19:38	363	off limb	
						14:29:49	163	off limb	
						14:41:35	506	off limb	
60	1997 Oct 1	Q1	22	−90	7:56:39	8:13:47			S
						8:30:53	84	off limb	
						8:47:40	261	off limb	
61	1997 Oct 1	Q2	23	−46	14:47:39	**15:21:39**			S
						15:38:38	56	off limb	
						15:56:08	36	off limb	
62	1997 Oct 1	Q1	22	−82	16:12:45	**16:29:39**			S
						16:43:06	131	off limb	
						17:12:24	87	off limb	
63	1997 Oct 3	Q3	15	−90	4:54:06	**5:12:32**			S
						5:26:04	49	off limb	
						5:35:14	206	off limb	
						5:54:13	121	off limb	
64	1997 Oct 3	Q2	23	−64	11:54:17	12:14:36			S
						12:29:29	108	109	
65	1997 Oct 6	Q0	−39	85	9:42:03	10:07:37			N
						10:22:38	169	off limb	
66	1997 Oct 9	Q3	24	−37	11:42:05	**11:56:53**			N
						12:19:18	149	267	
67	1997 Oct 10	Q1	24	−28	3:23:22	3:43:27			E
						4:00:52	85	102	
68	1997 Oct 11	Q4	26	−12	8:30:39	**8:47:41**			S
						9:04:40	123	123	
						9:21:47	126	128	
69	1997 Oct 12	Q4	−29	90	5:36:09	**5:54:53**			N
						6:11:39	214	off limb	
						6:28:40	275	off limb	
						6:46:21	254	off limb	
70	1997 Oct 20	Q2	13	8	6:31:59	**6:44:42**			S
						7:00:06	149	150	
71	1997 Oct 21	Q5	17	−7	16:18:36	17:34:51			S
						17:45:14	312	322	
						17:57:54	60	67	
						18:12:47	211	262	
						18:23:10	173	293	
72	1997 Oct 23	Q4	26	−6	13:14:38	13:29:28			S
						13:40:22	46	46	
						13:53:03	207	210	
						14:07:54	120	133	
						14:18:16	219	282	
73	1997 Oct 25	Q1	13	0	7:45:15	7:57:53			S
						8:12:43	93	96	
74	1997 Oct 29	Q1	34	8	7:21:53	7:38:48			N
						7:55:49	46	64	
						8:12:41	63	97	
75	1997 Nov 2	Q1	−17	1	2:49:45	**3:08:51**			NE
						3:25:09	174	177	

Table 3
(Continued)

	Date	Quality Rating	Source Location		Previous Image Time	Image Time	Speed		Direction of Measurement
			N/S	E/W			Plane-of-Sky	Projected	
76	1997 Nov 3	Q0	−18	16	4:31:54	5:02:19			N
		Note. Only one wavefront is shown in diagram; wavefronts are very inhomogeneous				5:19:04	See note		
						5:31:16			
77	1997 Nov 3	Q3	−18	18	8:46:59	**9:11:29**			N
						9:33:18	206	208	
78	1997 Nov 3	Q3	−18	18	10:21:14	**10:31:45**			N
						10:48:46	252	258	
79	1997 Nov 4	Q1	−18	29	5:57:01	6:13:54			N
						6:30:55	211	277	
80	1997 Nov 6	Q2 S	−19	61	11:39:00	**11:58:53**			E
						12:12:56	445	482	
						12:46:49	114	115	
81	1997 Nov 14	Q1	20	−81	9:34:17	9:50:53			S
						10:08:04	33	off limb	
						10:27:49	22	off limb	
82	1997 Nov 15	Q1	22	−61	22:33:56	**23:02:51**			S
						23:19:53	150	off limb	
83	1997 Nov 21	Q0	22	13	6:05:16	6:17:19			NE
						6:29:26	55	73	
						6:41:30	120	175	
						6:53:47	54	88	
84	1997 Nov 22	Q3	−19	9	11:42:15	12:08:58			N
85	1997 Nov 27	Q1	17	−65	13:11:10	13:36:58			
		Note. Only one wavefront is shown in diagram; evolution is very inhomogeneous				13:51:42	See note		
						14:03:36			
86	1997 Nov 28	Q1	−20	−14	11:45:03	12:18:43			NE
87	1997 Dec 12	Q2	−23	14	16:50:53	**17:05:53**			NE
						17:20:53	67	70	
						17:36:00	115	116	
88	1997 Dec 12	Q3	25	54	22:05:16	**22:21:53**			SW
89	1997 Dec 18	Q1	18	−14	12:21:20	12:37:46			S
						12:50:21	99	99	
90	1997 Dec 18	Q3	18	−14	13:49:41	**14:06:49**			S
		Note. Only two wavefronts are shown in diagram; third wavefront is very inhomogeneous				14:19:26	211	222	
						14:35:54	See note		
						14:48:30			
91	1997 Dec 18	Q2	18	−9	21:02:09	21:15:33			S
		Note. Only one wavefront is shown in diagram; other wavefronts are very inhomogeneous				21:32:27	See note		
						21:45:48			
92	1997 Dec 28	Q3	21	14	5:15:24	**5:22:58**			S
						5:33:27	223	230	
						5:44:20	149	150	
93	1997 Dec 30	Q1	−28	−27	5:36:30	5:44:01			N
						5:54:29	115	125	
94	1997 Dec 30	Q1	−29	−19	19:47:27	**19:58:23**			SW
		Note. Only two wavefronts are shown in diagram; third wavefront is very inhomogeneous				20:08:54	129	175	
						20:16:56	See note		
95	1998 Jan 3	Q1	−31	35	18:37:31	**18:50:00**			S
						19:07:08	72	80	
						19:30:05	27	47	
96	1998 Jan 3	Q0 S	20	17	22:12:48	22:29:21			S
						22:41:50	92	93	
						23:12:44	51	51	
97	1998 Jan 6	Q1	29	32	0:33:58	**0:51:17**			SW
						1:14:10	15	15	
						1:33:10	37	39	
98	1998 Jan 8	Q1	−26	−60	6:56:03	**7:18:55**			S
						7:37:43	69	off limb	
						7:54:53	20	off limb	
99	1998 Jan 12	Q2	−24	−15	2:00:30	**2:13:07**			N
		Note. Only two wavefronts are shown in diagram; third wavefront is very inhomogeneous				**2:29:36**	201	203	
						2:43:40	See note		
100	1998 Jan 14	Q2	16	−37	22:41:01	**23:09:37**			S
						23:29:39	98	99	
						23:42:00	269	272	

Table 3
(Continued)

	Date	Quality Rating	Source Location		Previous Image Time	Image Time	Speed		Direction of Measurement
			N/S	E/W			Plane-of-Sky	Projected	
101	1998 Jan 17	Q2	−24	62	22:33:08	**22:49:05**			S
						23:03:28	125	off limb	
						23:34:09	116	off limb	
102	1998 Jan 19	Q1	34	90	6:29:34	**6:43:40**			
						7:18:49	105	off limb	S
103	1998 Jan 20	Q3	23	−90	19:32:54	**19:51:12**			
						20:01:54	180	off limb	S
						20:19:00	152	off limb	
104	1998 Jan 25	Q4	27	−29	14:18:55	14:31:26			S
						14:47:53	239	240	
						15:01:57	150	158	
						15:20:08	116	134	
105	1998 Jan 25	Q0	−24	32	19:12:20	19:34:57			NW
						19:55:24	41	52	
						20:13:18	167	187	
106	1998 Jan 25	Q1	26	−53	21:24:45	**21:35:05**			S
						21:54:51	242	246	
						22:12:58	147	211	
107	1998 Jan 26	Q3	−25	42	22:21:21	**22:33:08**			N
						23:03:50	162	163	
108	1998 Jan 27	Q3	16	−22	22:02:54	**22:19:59**			SW
						22:34:02	181	182	
						23:04:45	94	101	
109	1998 Jan 29	Q0	24	90	15:51:11	16:03:09			S
						16:21:19	68	off limb	
110	1998 Feb 1	Q2	26	−90	18:54:01	**19:22:41**			S
						19:57:15	51	off limb	
111	1998 Feb 2	Q4	26	−90	17:32:36	**17:50:31**			S
						18:04:30	226	261	
						18:18:35	207	224	
						18:32:42	78	85	
112	1998 Feb 2	Q0	−31	−13	18:15:14	18:29:21			N
						18:43:21	43	45	
113	1998 Feb 10	Q2	28	−23	6:20:24	6:34:02			W
						6:51:03	56	70	
						7:14:12	97	133	
						7:34:20	33	54	
114	1998 Feb 18	Q1	−24	25	9:33:58	9:51:29			NW
						10:03:12	400	654	
115	1998 Feb 22	Q1	−18	−11	2:01:37	2:18:24			N
						2:32:27	71	71	
116	1998 Feb 23	Q2	−18	−90	12:17:49	**12:31:53**			S
						12:49:03	237	off limb	
117	1998 Feb 27	Q0	17	68	9:10:13	9:33:58			S
						9:51:17	165	off limb	
118	1998 Feb 28	Q1	−17	−21	0:15:02	**0:26:31**			NW
						0:40:18	237	239	
119	1998 Mar 4	Q1	−25	61	17:30:28	17:35:26			N
						17:40:24	324	334	
						17:45:22	310	313	
						17:50:04	446	484	
						17:55:00	433	439	
120	1998 Mar 7	Q2	−24	−65	6:07:22	**6:24:40**			N
						6:50:13	62	62	
121	1998 Mar 10	Q3	−26	−24	9:01:56	**9:27:29**			N
						9:54:16	96	105	
						10:12:26	167	215	
122	1998 Mar 11	Q0	−17	50	14:53:15	15:11:27			N
123	1998 Mar 13	Q2	−24	28	18:12:20	**18:23:58**			N
						18:36:01	166	171	
124	1998 Mar 13	Q3	−16	90	20:51:06	**21:01:41**			N
						21:12:45	305	345	
						21:23:13	280	282	
						21:34:56	108	121	

Table 3
(Continued)

	Date	Quality Rating	Source Location		Previous Image Time	Image Time	Speed		Direction of Measurement
			N/S	E/W			Plane-of-Sky	Projected	
125	1998 Mar 15	Q0	−14	−2	19:11:17	19:34:13			N
						19:47:43	367	425	
126	1998 Mar 27	Q3	31	−50	0:33:05	**0:44:01**			S
						1:06:47	210	213	
						1:27:17	218	219	
127	1998 Apr 16	Q0	−23	−67	20:18:54	20:35:43			NW
						20:55:57	93	107	
						21:05:16	230	243	
						21:18:58	157	162	
128	1998 Apr 20	Q2	−27	90	9:22:59	**9:34:47**			N
						9:57:51	333	off limb	
129	1998 Apr 21	Q1	−17	55	6:56:34	7:14:00			N
						7:39:39	44	46	
						8:01:51	37	39	
						8:20:41	91	91	
						8:32:23	200	210	
130	1998 Apr 22	Q2	24	−7	14:23:57	**14:40:40**			S
						14:53:50	72	77	
						15:09:36	68	70	
131	1998 Apr 23	Q4	−21	−90	5:33:35	**5:49:21**			NW
						6:01:36	293	402	
						6:19:33	195	218	
132	1998 Apr 25	Q2	−14	−90	0:53:20	**1:19:41**			N
						1:39:53	132	159	
133	1998 Apr 25	Q1	−14	−90	14:05:27	14:20:06			NW
						14:31:59	208	433	
134	1998 Apr 25	Q2	−14	−76	18:03:31	18:08:08			NW
						18:30:24	231	240	
135	1998 Apr 27	Q3	−22	−47	7:52:34	8:06:00			NW
						8:21:01	108	110	
						8:36:00	95	96	
						8:51:00	237	260	
136	1998 Apr 27	Q4	−20	−48	8:51:00	9:05:59			NW
						9:21:04	360	367	
						9:35:52	280	289	
137	1998 Apr 29	Q3	−17	−24	5:09:45	**5:22:09**			N
						5:36:15	199	215	
						5:52:25	180	240	
138	1998 Apr 29	Q1	−17	−22	8:03:47	8:18:47			NW
						8:34:02	176	178	
139	1998 Apr 29	Q5	−17	−15	16:02:56	**16:18:48**			NW
						16:34:20	194	199	
						16:51:55	235	282	
						17:03:41	160	266	
						17:18:48	74	182	
140	1998 Apr 30	Q1	−15	−8	21:36:25	**21:52:33**			NE
						22:04:08	259	307	
141	1998 May 1	Q0	−17	3	17:26:57	17:44:03			N
						17:59:32	94	95	
						18:17:53	114	118	
142	1998 May 1	Q3	−19	3	22:22:53	**22:39:54**			N
						22:56:56	220	225	
						23:32:55	166	188	
143	1998 May 2	Q1	−10	12	4:04:35	4:18:55			N
						4:35:59	82	84	
144	1998 May 2	Q2	−19	−7	4:53:39	5:07:52			NE
						5:22:32	175	180	
145	1998 May 2	Q0	−13	12	7:56:07	8:07:53			N
						8:20:30	175	176	
						8:34:33	101	105	
146	1998 May 2	Q3 S	−13	19	13:19:46	**13:40:12**			N
						14:10:21	296	438	
147	1998 May 2	Q1	−23	10	20:25:35	**20:37:53**			NE
						20:50:13	137	138	

Table 3
(Continued)

	Date	Quality Rating	Source Location		Previous Image Time	Image Time	Speed		Direction of Measurement
			N/S	E/W			Plane-of-Sky	Projected	
148	1998 May 3	Q0	−23	33	9:47:53	9:59:50			SE
						10:11:47	176	208	
						10:23:41	188	267	
						10:35:39	157	223	
149	1998 May 3	Q3	−12	35	21:09:24	**21:22:37**			N
						21:36:42	319	351	
						21:54:16	156	327	
150	1998 May 5	Q1	−16	51	8:09:34	**8:22:03**			N
						8:36:58	68	68	
						8:54:33	34	35	
151	1998 May 5	Q2	−15	67	23:23:59	**23:36:26**			N
						23:56:10	155	183	
152	1998 May 6	Q3 S	−17	68	7:58:28	**8:09:58**			NE
						8:22:34	327	359	
						8:38:05	139	140	
153	1998 May 8	Q2	−14	90	1:57:07	**2:08:53**			E
						2:21:27	203	372	
154	1998 May 8	Q2 S	−16	90	5:51:14	**6:03:02**			NE
						6:18:58	228	362	
						6:34:02	242	258	
155	1998 May 9	Q1 S	−16	90	1:44:08	2:03:32			NE
						2:15:16	188	230	
156	1998 May 9	Q2 S	−16	90	3:11:20	**3:28:56**			E
						3:42:53	131	343	
						4:02:24	221	299	
157	1998 May 9	Q2 S	−16	90	19:39:13	20:10:43			E
						20:23:14	134	296	
						20:43:01	246	307	
158	1998 May 11	Q1	−16	90	0:51:43	**1:17:36**			N
						1:41:09	28	37	
						1:57:35	75	81	
159	1998 May 19	Q3	26	47	9:32:25	**9:54:47**			S
						10:06:30	173	190	
						10:18:55	37	39	
160	1998 May 21	Q1	26	90	4:16:55	4:35:50			S
						5:05:52	75	83	
						5:18:18	70	77	
						5:32:26	104	117	
161	1998 May 25	Q3	−16	−42	3:02:12	**3:18:01**			N
						3:32:32	121	121	
						3:52:12	219	225	
162	1998 May 27	Q2	21	61	13:06:45	**13:32:29**			E
						13:53:08	227	227	
163	1998 May 29	Q0	19	90	21:27:23	**22:09:09**			S
						22:21:23	276	off limb	
164	1998 May 30	Q0 S	−24	−42	0:50:54	**1:16:48**			N
						1:37:32	142	143	
165	1998 Jun 3	Q0	15	90	11:32:58	**11:55:22**			S
						12:07:06	136	off limb	
166	1998 Jun 3	Q2	15	90	22:32:41	23:03:29			S
						23:18:19	165	off limb	
167	1998 Jun 4	Q2	24	−90	8:38:02	**8:55:31**			S
						9:09:29	159	off limb	
168	1998 Jun 4	Q0	−17	−50	11:17:21	**11:31:11**			NW
						11:53:13	205	212	
169	1998 Jun 4	Q0	−18	−49	14:51:58	15:03:49			NW
						15:17:21	418	437	
170	1998 Jun 8	Q2	−16	9	16:01:48	**16:17:54**			W
						16:33:56	208	241	
						16:50:08	157	241	
171	1998 Jun 10	Q1	22	64	14:33:27	**14:48:27**			NW
						15:00:14	77	off limb	
172	1998 Jun 11	Q4	14	−90	9:20:04	**9:35:07**			S
						9:59:48	67	off limb	
						10:09:31	345		
						10:20:03	784		
						10:34:57	380		

Table 3
(Continued)

	Date	Quality Rating	Source Location		Previous Image Time	Image Time	Speed		Direction of Measurement
			N/S	E/W			Plane-of-Sky	Projected	
173	1998 Jun 13	Q4	−23	5	15:23:33	**15:40:08**			NW
						15:53:45	258	271	
						16:02:44	170	207	
174	1998 Jun 16	Q1	29	90	4:37:59	**4:51:38**			S
						5:02:14	49	off limb	
						5:19:16	128		
						5:34:02	221		
175	1998 Jun 16	Q1	−27	90	18:02:18	**18:18:56**			N
						18:34:15	342	off limb	
176	1998 Jun 17	Q0	22	−30	Possible wave during data dropout between 02:43 and 05:07				

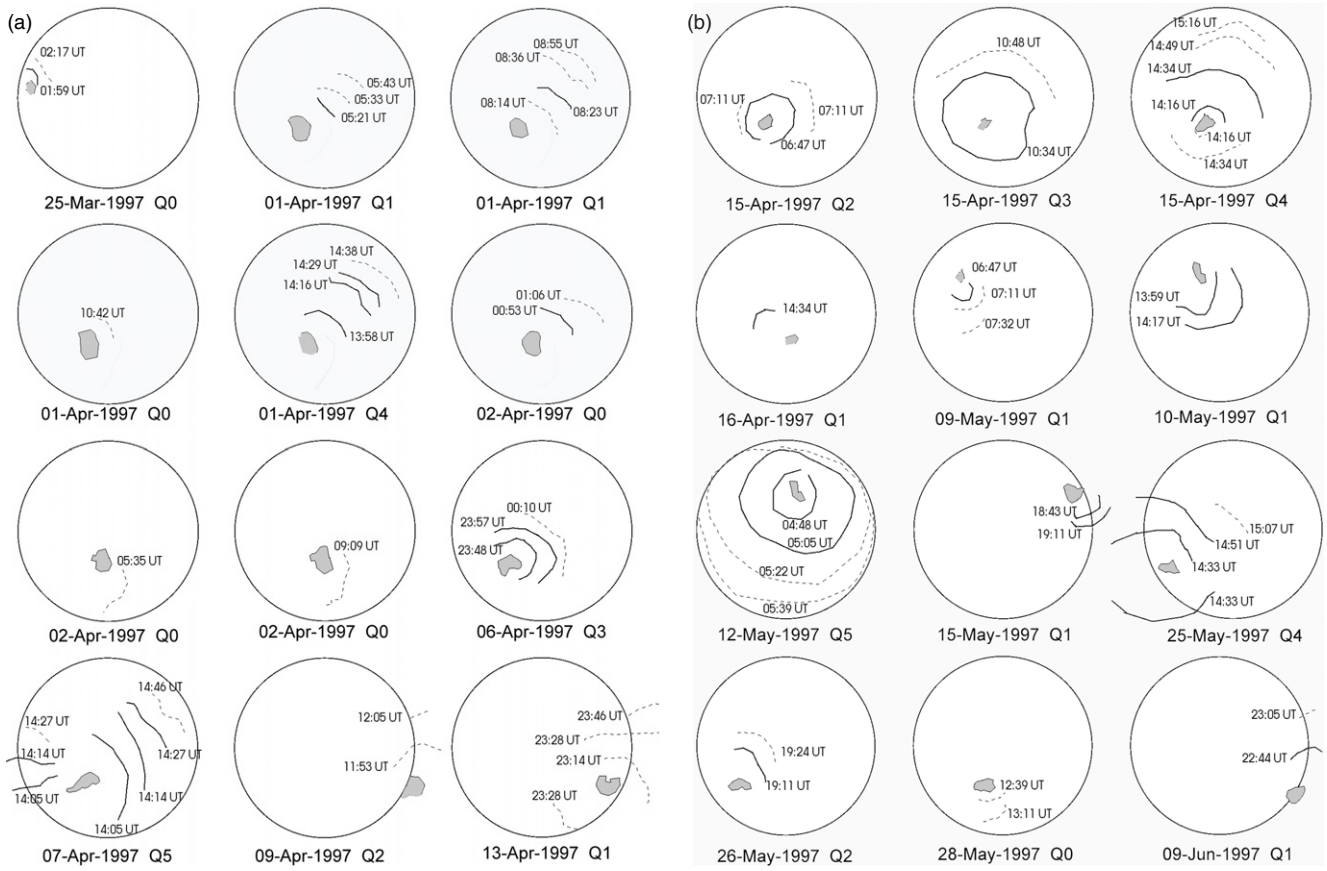

Figure 8. (a–o) Wave diagrams for each of the 176 entries in the catalog.

was observed in the EIT images. For this reason, we include in the catalog the times of the EIT images that contain the EIT wave, along with the time of the EIT image immediately before the appearance of the wave. The onset time of the wave lies somewhere between the pre-event image time and the time of the first image in the observation.

In the example listing in Table 1, the start time of the wave lies somewhere between the image times of 02:32 and 02:49 UT. Note: as mentioned previously, the date listed in the catalog corresponds to the time of the first wave image, and not the pre-event image.

2.6. Image Times

Each catalog entry consists of one line for each image in which the wave is observed. In Table 1, the first listing consists of two lines, one for each image, and the second listing consists of three. Correspondingly, there are two wave fronts shown in the summary image shown in the first frame of Figure 3, and three in the second.

The wave times in the catalog are listed fully, while the times on the images are truncated (therefore, the 1:59:35 UT image on 1997 March 25 is shown at 1:59 UT on the wave diagram in Figure 3). As described above, wave fronts which are clear and well defined are indicated with a solid line, while poorly resolved or faint fronts are indicated with a dashed line. The times in the catalog corresponding to the former case are shown in boldface.

Unfortunately, an instrumental effect adds to the uncertainty of the EIT wave times: the LASCO/EIT on board clock on *SOHO* runs fast, and there is an inaccuracy of at least 15 s

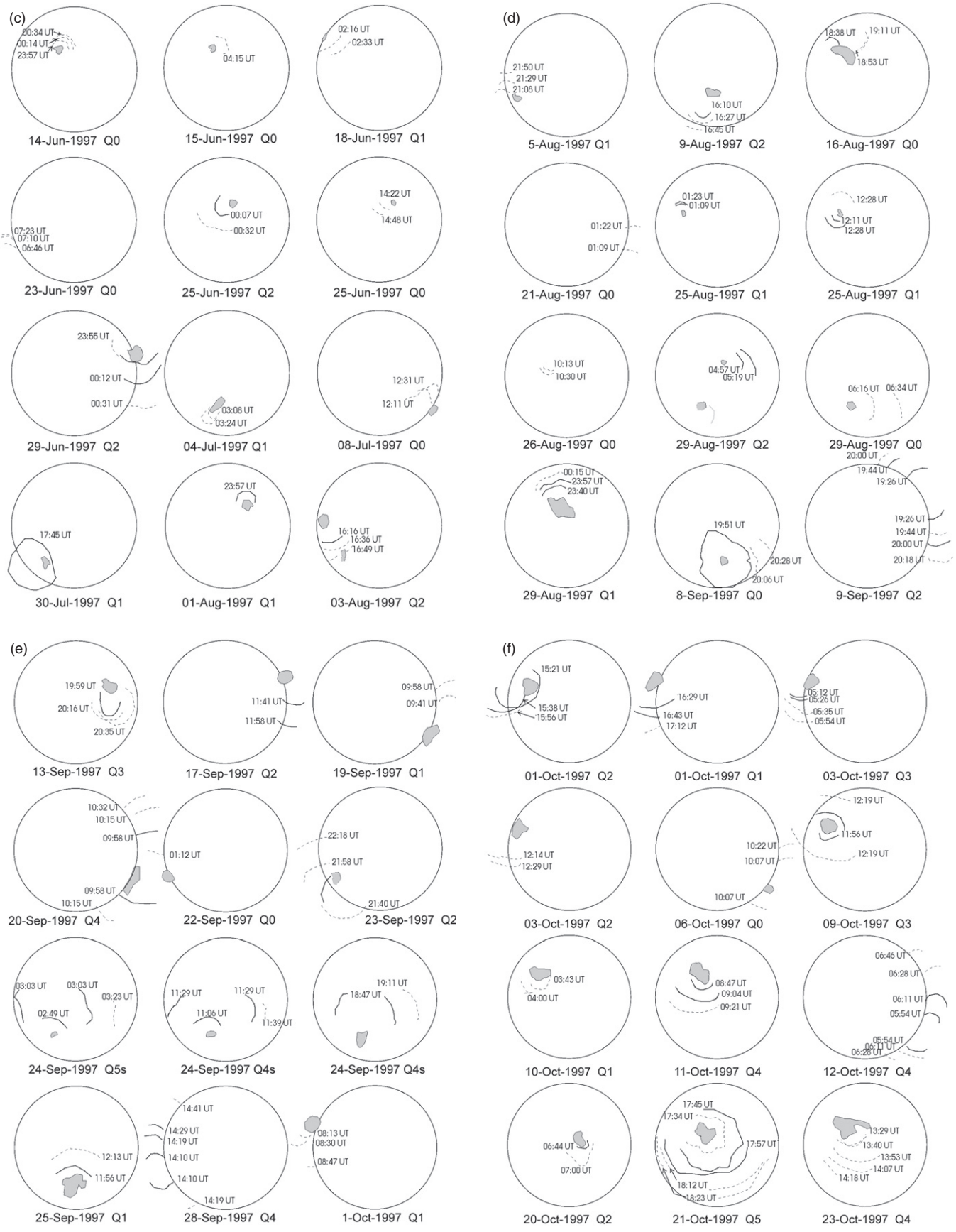

Figure 8. (Continued)

Figure 8. (Continued)

Figure 8. (Continued)

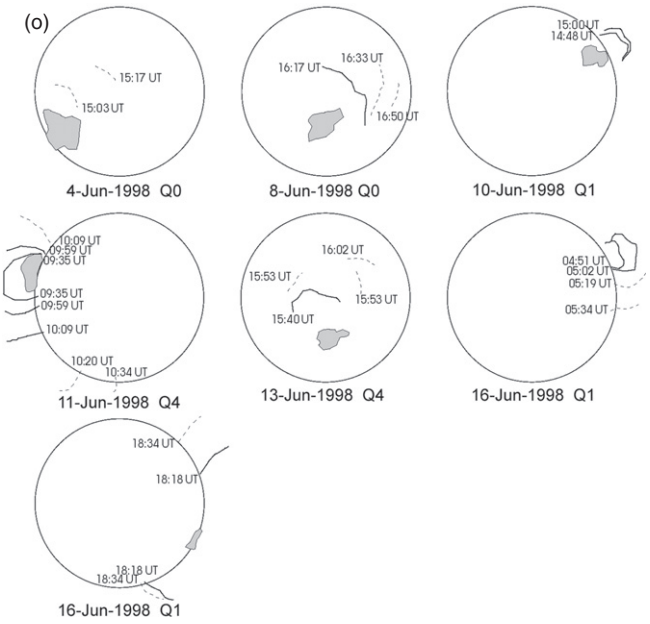

Figure 8. (Continued)

associated with this problem. Beginning in 1997 September, regular time corrections based on a record of the time offset became available. The image times prior to 1997 September have been provided by a time correction algorithm developed by A. Vourlidas.

It is important to mention that several papers that have been published have listed image times which are different from the entries in this catalog. This is because the time correction algorithm was not available at the time. For example, the time of the EIT images for 1997 April 7 given in Thompson et al. (1999) are 7 minutes later than the times listed in this catalog. In the paper, an extrapolation of the wave locations placed the intersection of the wave centroid with the flaring active region at 13:50 UT, while the current image times would give 13:43 UT.

2.7. Plane-of-Sky Speed

The speed of the waves is determined based on the location of the wave front and the image times. Therefore, only events with two or more images have a speed listed in the catalog. The numbers listed in the catalog represent the speed along one propagation path near the area of the maximum density increase, and if there are N images listed in the catalog entry, $N - 1$ speeds will be given. The Plane-of-Sky speed listed in the catalog is calculated relative to a single pair of points chosen to "represent" the motion of the wave front. As discussed in Thompson et al. (1999), wave fronts do not necessarily travel in a radial or coplanar manner, so different speeds can be derived at different points along the same wave front. Wills-Davey & Thompson (1999) demonstrate this effect more explicitly.

This portion of the catalog is called the "Plane-of-Sky" speed because the speed derived from this measurement does not take into account the curvature of the Sun, nor does it assume any propagation varying with time or height. It merely reflects the distance of a straight line between the two data points, divided by the times between the images.

2.8. Projected Speed

While the "Plane-of-Sky" speeds are relatively accurate for measurements taken near disk center, the true distance traveled by the wave is grossly underestimated for measurements approaching the limb of the Sun. Therefore, a second "Projected" speed is given in the catalog, which re-calculates the speed assuming the wave travels in a great circle along the Sun's photosphere.

This results in a more accurate estimate of the wave speed, but it still is not reliable. In addition to the inaccuracy introduced by inhomogeneous propagation in space and time, these waves are observed in the Sun's corona, not the photosphere, resulting in a chronic underestimation of the speed.

Throughout the catalog, there are entries where the words "off limb" appear in place of a number in the Projected Speed column. These wave fronts were measured above the limb of the Sun, in which case the Plane-of-Sky speed is a more accurate representation of the wave speed.

We stress that the speeds in the catalog are available only for sampling purposes, and that they only represent the speed of the wave front along a single vector, measured where the wave is most observable (low corona), projected either against the plane of the sky or along a great circle of radius $= 1\ R_{\rm Sun}$. Certainly, EIT is unable to resolve speed variations with timescales less than the EIT cadence. There is evidence from other sources of data that, particularly in the early stages of propagation, the wave speed can decrease significantly (Wills-Davey & Thompson 1999; Thompson et al. 2000). Therefore, the actual speed of the wave at the time of the first image can be much larger (by whole factors!) than the speed implied by the distance between the first and second images. Additionally, if the EIT image cadence is slower than 10 minutes per image, a wave with a speed exceeding 1000 km s^{-1} will have traveled a distance of one solar radius between images, making observations of multiple wave fronts unlikely.

2.9. Direction of Measurement

This portion of the catalog reflects the direction between two sampled points which were used to calculate the speeds. Please refer to the individual wave diagrams for a full assessment of the direction(s) of wave propagation.

3. CONCLUSION: USING THE CATALOG

Table 3 contains the full EIT wave catalog, and the diagrams corresponding to each entry are contained in Figure 8. The purpose of this wave catalog is to provide a reference for studies involving EIT wave phenomena and their association with other solar and heliospheric phenomena. Therefore, we have made efforts in the development of this catalog to provide for a wide range of research topics and interests.

As mentioned previously, there will be many "EIT wave" transients that are not listed in the catalog. These waves may have too low amplitude to be observed, or the times of the EIT observations may not have been optimal, or there may not be EIT data at all. Interruptions in the EIT image cadence of an hour or more happen on a fairly regular basis, so it's likely that a number of potentially excellent wave events are missing from the catalog.

Quality Ratings were introduced so that users of this catalog can take this into consideration when performing research based on entries in this catalog. A low-quality rating may imply that the wave had an extremely low amplitude, or it may have been a "false positive" associated with some other (non-wave) source of moving brightening. Therefore, a theorist interested in modeling wave propagation may want to focus only on entries

with Quality Ratings "Q4" or "Q5." Similarly, Biesecker et al. (2002), in determining the fraction of EIT waves emanating from regions which also produced a CME, found that the correlation improved greatly when the sample was restricted to "Q4" and "Q5" events. Including "false positive" entries in the Biesecker study can mislead one into believing that there was a higher percentage of EIT waves with no associated CME observation. In contrast, Klassen et al. (2000), determined the percentage of Type II radio bursts with EIT waves. A number of the Type II bursts in this study were associated with waves that had a low Quality Rating. Excluding all low-quality waves from the Klassen study would have resulted in a number of the Type II events also being excluded from the study. Therefore, the Quality Ratings and other fields in this catalog may be utilized to assist the reader in identifying which entries are most relevant to their research.

The authors thank M. J. West, C. E. Deforest, D. A. Biesecker, H. R. Gilbert, and J. B. Gurman for valuable discussion. The authors also thank the referees of this paper for their exceptional effort.

REFERENCES

Banerjee, D., Erdélyi, R., Oliver, R., & O'Shea, E. 2007, Sol. Phys., 246, 3
Biesecker, D. A., Myers, D. C., Thompson, B. J., Hammer, D. M., & Vourlidas, A. 2002, ApJ, 569, 1009
Chen, P. F., Wu, S. T., Shibata, K., & Fang, C. 2002, ApJ, 572, L99
Delaboudinière, J.-P., et al. 1995, Sol. Phys., 162, 291
Dere, K. P., et al. 1997, Sol. Phys., 175, 601
Eto, S., et al. 2002, PASJ, 54, 481
Handy, B. N., et al. 1999, Sol. Phys., 187, 229
Howard, R. A., et al. 2008, Space Sci. Rev., 136, 67
Klassen, A., Aurass, H., Mann, G., & Thompson, B. J. 2000, A&AS, 141, 357
Long, D. M., Gallagher, P. T., McAteer, R. T. J., & Bloomfield, D. S. 2008, ApJ, 680, L81
Ma, S., Lin, J., Chen, P., & Chen, H. 2009, in Proc. 10th Asian-Pacific Regional IAU Meeting, ed. I. F. Corbett et al. (Cambridge: Cambridge University Press)
Moreton, G. E. 1960, AJ, 65, 494
Moreton, G. E., & Ramsey, H. E. 1960, PASP, 72, 357
Ofman, L., & Thompson, B. J. 2002, ApJ, 574, 440
Podladchikova, O., & Berghmans, D. 2005, Sol. Phys., 228, 265
Pohjolainen, S., et al. 2001, ApJ, 556, 421
Smith, S. F., & Harvey, K. L. 1971, in Physics of the Solar Corona, ed. C. J. Macris (Dortrecht: Reidel), 156
Thompson, B. J., et al. 1998, Geophys. Res. Lett., 25, 2465
Thompson, B. J., et al. 1999, ApJ, 517, L151
Thompson, B. J., et al. 2000, Sol. Phys., 193, 161
Uchida, Y. 1968, Sol. Phys., 4, 30
Uchida, Y. 1970, PASJ, 22, 341
Uchida, Y. 1974, Sol. Phys., 39, 43
Vršnak, B., Warmuth, A., Brajsa, R., & Hanslmeier, A. 2002, A&A, 394, 299
Wang, Y.-M. 2000, ApJ, 543, L89
Warmuth, A., Vršnak, B., Aurass, H., & Hanslmeier, A. 2001, ApJ, 560, L105
Warmuth, A., Vršnak, B., Magdalenić, J., Hanslmeier, A., & Otruba, W. 2004a, A&A, 418, 1101
Warmuth, A., Vršnak, B., Magdalenić, J., Hanslmeier, A., & Otruba, W. 2004b, A&A, 418, 1117
Wills-Davey, M. J. 2006, ApJ, 645, 757
Wills-Davey, M. J., & Thompson, B. J. 1999, Sol. Phys., 190, 467
Wu, S.-T., et al. 2001, J. Geophys. Res. A, 11, 25089
Zhukov, A. N., & Auchere, F. 2004, A&A, 427, 705